International Journal of the Physical Sciences Vol. 6(15), pp. 3662-3671, 4 August, 2011
Available online at http://www.academicjournals.org/IJPS
DOI: 10.5897/IJPS10.116
ISSN 1992 - 1950 ©2011 Academic Journals

Full Length Research Paper

Nano sized copper particles by electrolytic synthesis and characterizations

T. Theivasanthi* and M. Alagar

Centre for Research and Post Graduate Department of Physics, Ayya Nadar Janaki Ammal College (Autonomous), Sivakasi-626124, Tamilnadu, India.

Accepted 20 June, 2011

This work reports a simple, novel, cost effective and eco-friendly electrolytic synthesis of copper nanoparticles using copper sulphate as metal precursor. The synthesis rate is much faster than other methods and this approach is suitable for large scale production. They are characterized by X-ray diffraction (XRD); scanning electron microscope and Fourier transform-infra red (FT-IR) techniques to analyze size, morphology and functional groups. XRD studies reveal a high degree of crystallinity and monophasic nature of copper nanoparticles. Their particle size is found to be 24 nm and specific surface area (SSA) is 28 m^2/g. SSA analysis of copper nanoparticles reports that increasing their SSA improves their antibacterial actions. Microbiology essay finds that copper nanoparticles are effective against *Escherichia coli* and *Bacillus megaterium* bacteria. SSA of bacteria analysis reveals that it plays a major role while on reactions with antimicrobial agents.

Key words: X-ray diffraction (XRD), copper nanoparticles, Williamson Hall plot, electrolysis, Debye-Scherrer.

INTRODUCTION

New class of materials has been creating a technological revolution in the last decade. The synthesis of new materials made of particles, rods and wires with dimensions in the nanometer scale is among the most active areas of research in science due to the novel and unique properties of these materials compared to conventional materials made from micron sized particles. Copper nanoparticles have received considerable attention owing to their attractive physicochemical properties. In addition, they exhibit strong toxicity various microorganisms are well known and have shown to be a promising antimicrobial material.

In nanoparticles preparation, it is very important to control the particle size, particle shape and morphology. The characters of metal nanoparticles like optical, electronic, magnetic, catalytic and biological related activities are depending on their sizes, shapes and chemical surroundings. The properties of such materials can be engineered by controlling the dimensions via physical, chemical or biological methods.

Most of the existing synthesizing methods of metal nanoparticles are complicated, require specific equipments and produce only small amounts of nanomaterials. Metallic nanoparticles are traditionally synthesized by wet chemical methods where the chemicals used are often toxic and flammable. Likewise, there are lots of difficulties in biosynthesis methods to separate the synthesized nanoparticles from the bio-chemical precursors, impurity contents mixed in the precursors. Also, these end products have short duration of life period.

Discussions about easy, simple, fast and low cost preparation that is, electrolysis synthesis of copper nanoparticles and its characterizations [X-ray diffraction (XRD), scanning electron microscope (SEM) and Fourier transform-infra red (FT-IR)] are studied in this research paper. This method can be used to prepare wide range of materials. The synthesized nanoparticles size is 24 nm. Also, in this paper we report changes in SSA of copper nanoparticles, its effects on antibacterial activities and roles of bacteria SSA while reacting with copper nanoparticles.

*Corresponding author. E-mail: theivasanthi@pacrpoly.org.

Abbreviations: SSA, specific surface area; **ZOI,** standard zone of inhibition; **FCC,** face centered cubic symmetry; **h k l,** Miller Indices; **JCPDS,** Joint Committee on Powder Diffraction Standards; **MTPs,** multiply twinned particles; **TEM,** transmission electron microscopy.

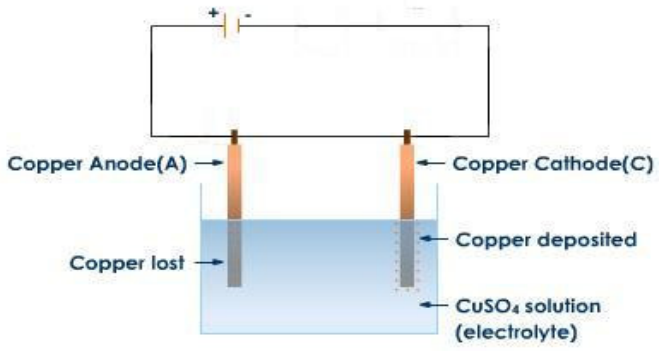

Figure 1. Electrolysis of copper sulphate solution.

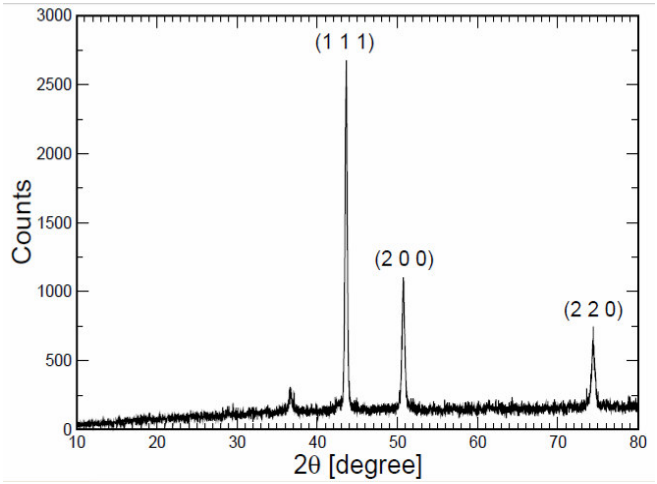

Figure 2. XRD showing peak indices and 2 θ positions.

EXPERIMENTAL METHODOLOGY

Chemical effects of current

The phenomenon of electrolysis is an important chemical effect of electric current. It passes and conducts electric current through an electrolyte solution together with the resulting chemical changes. It is the dissociation process of an electrolyte and the dissociated ions that appear at the two electrodes. Electrolytes are conducting electricity due to drifting of ions (positive cations and negative anions).

Solid $CuSO_4$ is made up of Cu_2^+ and SO_4^- ions bound by a strong force of attraction. The thermal energy at room temperature is only 0.03 eV per molecule which is not enough to dissociate $CuSO_4$ into Cu_2^+ and SO_4^- ions. When $CuSO_4$ is dissolved in water, the force of attraction is greatly reduced because of the high dielectric constant (= 81) of water. In fact, the force reduces by a factor of 81, and the thermal energy is sufficient for the ionization process that is to dissociate $CuSO_4$ completely into Cu_2^+ and SO_4^- ions.

Electrolytic conduction phenomenon

When a steady current flow into the electrolytic cell, due to ionization process, the $CuSO_4$ solution is dissociated, copper is removed from the anode and deposited on the cathode. Electrons flow from the negative terminal to the cathode, the Cu^{2+} ions move towards cathode and the SO_4^{2-} ions move towards anode. Oxidation reaction takes place at the anode and reduction reaction occurs at the cathode, and Cu atoms get deposited at the cathode. Copper has valency two and two electrons circulate for the deposition of one copper atom.

$$CuSO_4 \longrightarrow Cu^2 + SO_4^{2-} \quad (1)$$

$$Cu + SO_4^{2-} \longrightarrow Cu^{2+} SO_4^{2-} + 2e^- \quad (2)$$

$$Cu^{2+} + 2e^- \longrightarrow Cu \quad (3)$$

Electrolysis synthesis

Electrolysis method was adopted for copper nanoparticles preparation. Copper sulphate salt ($CuSO_4.5H_2O$) was kept in an electrolytic cell (consists of a cleaned glass vessel, two copper electrodes and direct current (DC) power supply unit), distilled water was poured, stirred well and a homogenous aqueous copper sulphate solution was made. Surface-cleaned copper electrodes are connected with positive (Anode) and negative (cathode) of DC Power Supply unit (15 volt and 6 ampere) separately on one end, inserted in the copper sulphate solution on another end. Electrolysis of this solution was done by passing constant current inside solution through anode and cathode. This process is shown in Figure 1. At the end of electrolyzing process, copper nanoparticles deposition on the cathode surface was observed, they were removed carefully from the cathode surface and copper nanoparticles was collected. Its appearance was very fine and powdery in nature. Its structural characterizations were studied and results confirmed the formation of copper nanoparticles.

XRD analysis of the prepared sample of copper nanoparticles was done using a Rigaku Ultima III X-Ray Diffractometer, Cu-Kα X-rays of wavelength (λ) = 1.54056 Å and data was taken for the 2θ range of 10 to 80° with a step of 0.02°. The surface morphology were analyzed by using SEM Model S-3000H of HITACHI. Functional groups were analyzed by SHIMADZU FT-IR spectrometer. The antibacterial activities of copper nanoparticles were studied against *E. coli* and *B. megaterium* by Agar disc diffusion method. Standard zone of inhibition (ZOI) was measured and evaluated from this microbiology assay.

RESULTS AND DISCUSSION

X-ray diffraction (XRD) studies - Peak indexing

The XRD pattern of the copper nanoparticles synthesized by electrolysis method is shown in Figure 2. Indexing process of powder diffraction pattern is done and Miller Indices (h k l) to all peaks is assigned in first step. Indexing is done in two different methods and data are in Tables 1 and 2. Both of these methods bring the same results. In Table 1, it needs to find a dividing constant. The values in the 3rd column become integers (approximately). Here, the constant is 46 (= 184–138).

Table 1. Simple peak indexing.

Peak position (2θ)	1000×Sin^{2}θ	1000×Sin^{2}θ/46	Reflection	Remark
43.64	138	3	(1 1 1)	$1^2+1^2+1^2 = 3$
50.80	184	4	(2 0 0)	$2^2+0^2+0^2 = 4$
74.42	366	8	(2 2 0)	$2^2+2^2+0^2 = 8$

Table 2. Peak indexing from d-spacing.

2θ	d (Å)	1000/d^2	(1000/d^2)/77.32	hkl
43.64	2.073	232.07	3.01	111
50.80	1.796	310.02	4.01	200
74.42	1.274	616.11	8.00	220

Table 3. Experimental and standard diffraction angles of copper specimen.

Experimental diffraction angle [2θ in degrees]	Standard diffraction angle [2θ in degrees] JCPDS Copper: 04-0836
43.640	43.297
50.800	50.433
74.420	74.130

Table 4. Ratio between the intensities of the diffraction peaks.

Diffraction peaks	Sample value	Conventional value
(200) and (111)	0.41	0.46
(220) and (111)	0.27	0.20

A number of strong Bragg reflections can be seen which correspond to the (111), (200) and (220) reflections of face centered cubic symmetry (FCC) copper. Any spurious diffraction which indicating the crystallographic impurities is not found. Each crystallographic facet contains energetically distinct sites based on atom density. The copper nanoparticles contain high atom density facets such as (111) that are known to be highly reactive (Ruparelia et al., 2008). The high intense peak for FCC materials is generally (111) reflection, which is observed in the sample. For FCC, each h, k, l should be all even or all odd number which is also observed.

The remarkably intensive diffraction peak noticed at 2θ value of 43.64 from the {111} lattice plane unequivocally indicates that their basal plane which is the top crystal plane, should be the {111} plane. It has been suggested that this plane may possess lowest surface tension (Parameswari et al., 2010). The intensity of peaks reflects the high degree of crystallinity of the copper nanoparticles. However, the diffraction peaks are broad which indicates that the crystallite size is very small (Irshad et al., 2011). The XRD shows that Cu nanoparticles formed are crystalline. The size of the Cu nanoparticles estimated from Debye-Scherrer formula (Instrumental broadening) is 24 nm.

Three peaks at 2θ values of 43.64, 50.80, and 74.42 deg corresponding to (111), (200) and (220) planes of copper is observed and compared with the standard powder diffraction card of Joint Committee on Powder Diffraction Standards (JCPDS), copper file N0. 04-0836. The XRD study confirms/indicates that the resultant particles are FCC copper nanopowder. The experimental diffraction angle [2θ] and standard diffraction angle [2θ] of Cu specimen in the Table 3 are in agreement (Das et al., 2009).

It is worth noting that the ratio between the intensities of the (200) and (111) diffraction peaks, and (220) and (111) peaks enumerated in Table 4 is also close with the conventional value (0.41 versus 0.46) and (0.27 versus 0.20) (Yugang and Younan, 2002).

X-ray diffraction (XRD)-lattice constant

The FCC crystal structure of copper has unit cell edge '*a*'= 3.62 Å and this value is calculated theoretically by

Table 5. The grain size of copper nanopowder.

2θ of the intense peak (deg)	hkl	FWHM of intense peak (β) radians	Size of the partcle (D) nm	d-spacing nm	Lattice parameter (*a*) Å
43.64	(111)	0.0059	25.32	0.2073	3.5905
50.80	(200)	0.0066	23.26	0.1796	3.5920
74.42	(220)	0.0070	24.88	0.1274	3.6034

Table 6. The lattice plane and the lattice spacing-d of XRD diffraction.

hkl	111		200		220	
	Experiment	Expected	Experiment	Expected	Experiment	Expected
d (Å)	2.073	2.090	1.796	1.810	1.274	1.279
2θ (deg)	43.64	43.23	50.80	50.35	74.42	74.03

using formula:

$$a = 4/\sqrt{2} \times r \quad (4)$$

For copper r = 128 pm. The experimental lattice constant '*a*' is calculated from the most intense peak (111) of the XRD pattern is 3.59 Å. Both theoretical and experimental lattice constant '*a*' are in agreement. The details of '*a*' value of all peaks have been produced in Table 5.

X-ray diffraction (XRD)-particle size calculation

From this study, considering the peak at degrees, average particle size has been estimated by using Debye-Scherrer formula,

$$D = \frac{0.9\lambda}{\beta cos\theta} \quad (5)$$

Where 'λ' is wave length of X-ray (0.1541 nm), 'β' is full width at half maximum (FWHM), 'θ' is the diffraction angle and 'D' is particle diameter size. The calculated particle size details are in Table 5. The value of d (the interplanar spacing between the atoms) is calculated using Bragg's Law.

$$2dsin\theta = n\lambda \quad (6)$$

X-ray diffraction (XRD)-expected 2θ positions

The expected 2θ positions of the first three peaks in the diffraction pattern and the interplanar spacing *d* for each peak are calculated using the following formulas and the details are shown in Table 6. The expected 2θ and d values are close with the experimental 2θ and d values.

$$1/d^2 = (h^2 + k^2 + l^2)/a^2 \quad (7)$$

Bragg's Law is used to determine the 2θ value:

$$\lambda = 2d_{hkl}sin\theta_{hkl}$$

X-ray diffraction (XRD) - Instrumental broadening

When particle size is less than 100 nm, appreciable broadening in XRD lines will occur. Diffraction pattern will show broadening because of particle size and strain. The observed line broadening will be used to estimate the average size of the particles. The total broadening of the diffraction peak is due to the sample and the instrument. The sample broadening is described by

$$FW(S) \times cos\theta = \frac{K \times \lambda}{Size} + 4 \times Strain \times sin\theta \quad (8)$$

The total broadening β_t is given by the equation

$$\beta_t^2 \approx \{\frac{0.9\lambda}{Dcos\theta}\}^2 + \{4\varepsilon tan\theta\}^2 + \beta_0^2 \quad (9)$$

ε is strain and β_0 instrumental broadening. The average particle size D and the strain ε of the experimentally observed broadening of several peaks will be computed simultaneously using least squares method. Instrumental broadening is presented in Figure 3.

Williamson and Hall proposed a method for deconvoluting size and strain broadening by looking at the peak width as a function of 2θ. Here, Williamson-Hall plot is plotted with sin θ on the x-axis and $_{\beta}$ cos θ on the y-axis (in radians). A linear fit is obtained for the data. From the linear fit, particle size and strain are extracted from y-intercept and slope respectively. The extracted particle size is 24 nm and strain is 0.00005. Figure 4

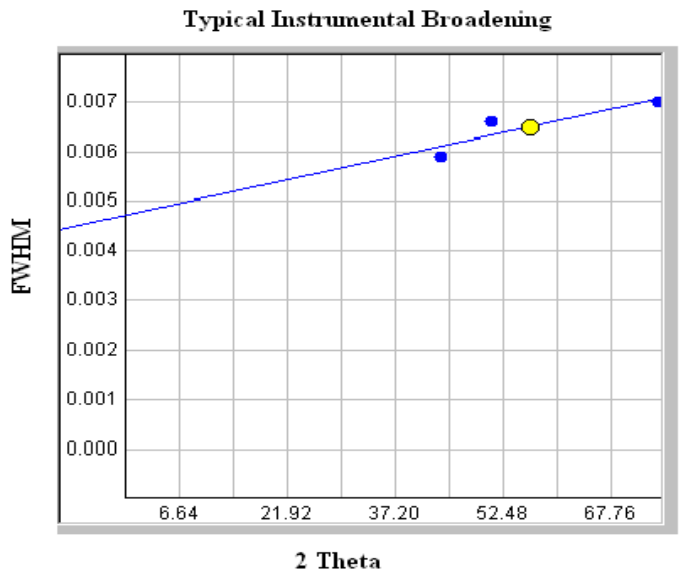

Figure 3. Typical instrumental broadening. y = -0.0000310x + 0.0048.

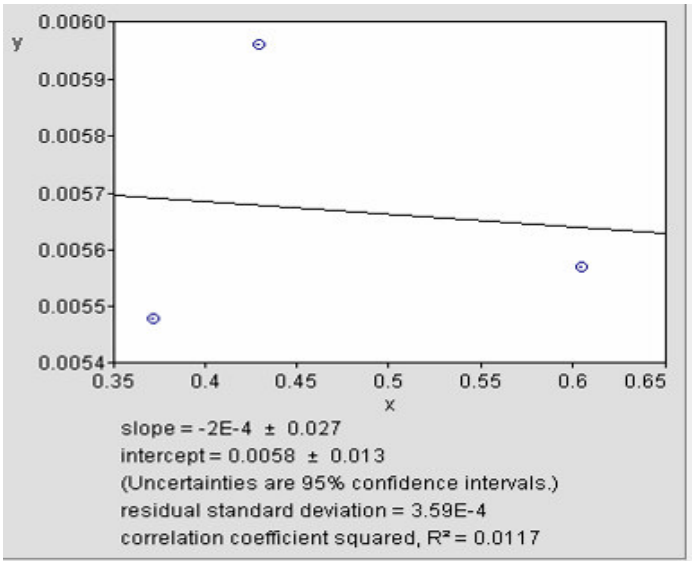

Figure 4. Williamson Hall plot is indicating line broadening value due to the equipment.

shows Williamson Hall plot.

Line broadening analysis is most accurate when the broadening due to particle size effects is at least twice the contribution due to instrumental broadening. The size range is calculated over which this technique will be most accurate. A rough upper limit is estimated for reasonable accuracy by looking at the particle size that would lead to broadening equal to the instrumental broadening. For example, for Monochromatic Lab X-ray (Cu Kα FWHM ~ 0.05° at 20° 2θ), the accurate size range is < 90 nm (900 Å) and the rough upper limit is = < 180 nm (1800 Å).

X-ray diffraction (XRD) - Crystallinity index

It is generally agreed that the peak breadth of a specific phase of material is directly proportional to the mean crystallite size of that material. Quantitatively speaking, sharper XRD peaks are typically indicative of high nanocrystalline nature and larger crystallite materials. From our XRD data, a peak broadening of the nanoparticles is noticed. The average particle size, as determined using the Scherrer equation, is calculated to be 24 nm. Crystallinity is evaluated through comparison of crystallite size as ascertained by SEM particle size determination. crystallinity index equation is presented below:

$$I_{cry} = \frac{D_p(SEM,TEM)}{D_{cry}(XRD)} (I_{cry} \geq 1.00) \quad (10)$$

Where I_{cry} is the crystallinity index; D_p is the particle size (obtained from either transmission electron microscopy (TEM) or SEM morphological analysis); D_{cry} is the particle size (calculated from the Scherrer equation). Table 7 displays the crystallinity index of the sample that scored higher than 1.0. The data indicate that the copper metal is highly crystalline and FCC phase structure is well-indexed. If I_{cry} value is close to 1, then it is assumed that the crystallite size represents mono-crystalline whereas a polycrystalline have a much larger crystallinity index (Xubin et al., 2010).

X-ray diffraction (XRD)-specific surface area (SSA)

SSA is a material property. It is a derived scientific value that can be used to determine the type and properties of a material. It has a particular importance in case of adsorption, heterogeneous catalysis and reactions on surfaces. SSA is the *SA* per mass.

$$SSA = \frac{SA_{part}}{Vpart * density} \quad (11)$$

Here *V part* is particle volume and SA_{part} is surface area of particle (Jiji et al., 2006).

$$S = 6 * 10^3 / D_p \rho \quad (12)$$

Where *S* is the specific surface area, *Dp* is the size of the particles, and *ρ* is the density of Cu 8.93 g/cm^3 (Jo-Yong et al., 2006). Mathematically, SSA can be calculated using these formulas. Both of these formulas yield the same result. Calculated value of SSA of the prepared copper nanoparticles is 28 m^2/g.

X-ray diffraction (XRD)-unit cell parameters

Unit cell parameters values calculated from XRD are enumerated in Table 8.

Table 7. The crystallinity index of copper nanoparticles.

Sample	Dp (nm)	Dcry (nm)	Icry (unitless)	Particle type
Copper Nanoparticles	98	24	~4.08	Polycrystalline

Table 8. XRD parameters of copper nanoparticles.

Parameter	Value
Structure	FCC
Space group	Fm-3m (Space group number: 225)
Point group	m3m
Packing fraction	0.74
Symmetry of lattice	cubic close-packed
Particle size	24 nm
Bond Angle	$\alpha = \beta = \gamma = 90^{\circ}$
Lattice parameters	$a = b = c = 3.59$ Å
Vol.unit cell(V)	46.268 $Å^3$
Radius of Atom	128 pm
Density (ρ)	8.93 g/cm^3
Mass	63.546 amu

Scanning electron microscope (SEM) morphological studies of copper nanoparticles

The results of SEM morphological and nanostructural studies are shown in Figure 5. It indicates that mono-dispersive and highly crystalline copper nanoparticles are obtained. The appearance is spherical in shape. The observations of some larger nanoparticles are composed of Van Der Waals clusters of smaller entities. From geometry, it is clear that the sizes of small individual particles are less than 100 nm in diameter, while the composite particles in lower resolution would appear higher in particle size.

Generally, on the nanometer scale, metals (most of them are FCC) tend to nucleate and grow into twinned and multiply twinned particles (MTPs) with their surfaces bounded by the lowest-energy {111} facets. Also, they may be attributed to the fact that Cu nanoparticles have the tendency to agglomerate due to their high surface energy and high surface tension of the ultrafine nano-particles. The fine particle size will result in a large surface area that will in turn, enhance the nanoparticles catalytic activity.

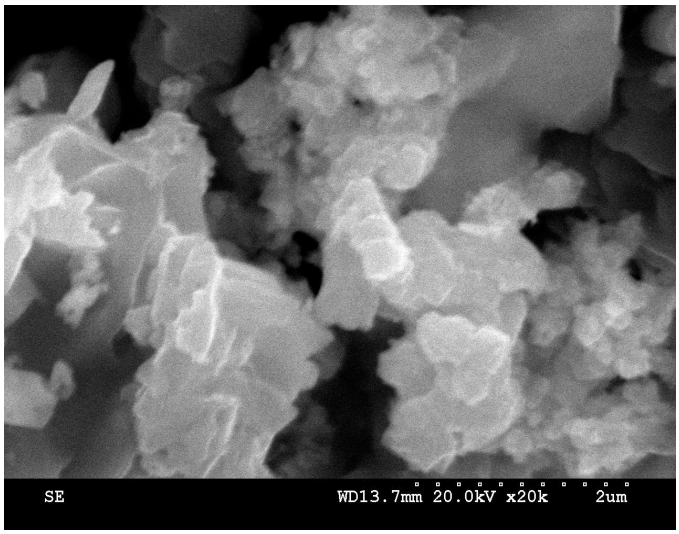

Figure 5. SEM picture showing copper nanoparticles.

Fourier transform-infra red (FT-IR) Analyses of Copper nanoparticles:

FT-IR spectroscopic studies were carried out to investigate the plausible mechanism behind the formation of these copper nanoparticles and offer information re-garding the functional groups. The representative spectra of copper nanoparticles are shown in Figure 6. Vibrational assignments/functional groups corresponding to the absorption peaks are enumerated in Table 9. A broad peak at 3439, weak peaks at 2813, 765, very weak peaks at 2727, 1126, medium peaks at 1383, 620, very strong absorption peak at 1594 and the strong absorption peaks at 1350, 1629 are observed. The peaks at 620, 725, 1126, 1350 represents the presence of S, SO_2 which may be from copper sulphate ($CuSO4.5H_2O$) solution, the metal precursor involved in the copper nanoparticles synthesis process.

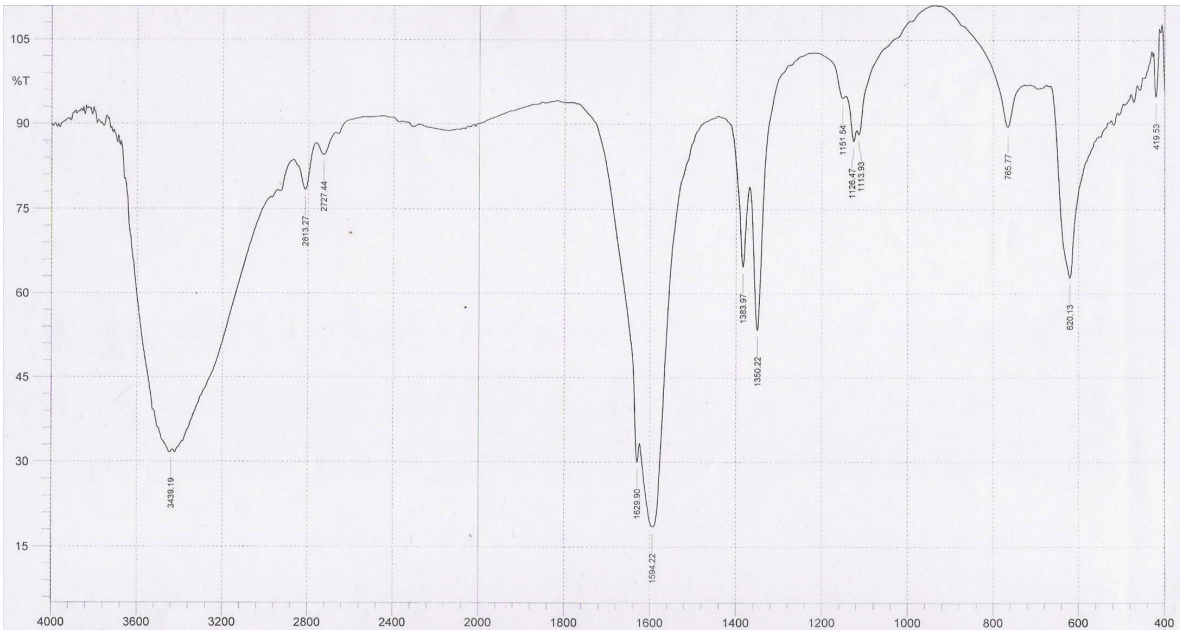

Figure 6. Wave number (cm^{-1}) of dominant peaks obtained from FT-IR absorption spectra.

Table 9. FTIR functional groups analyses.

Vibrational assignment/functional groups	Observed wave number (cm^{-1})	Visible intensity
N-Hγ	3439.19	Broad
CH_3 γ + CH_2 γ_s	2813.27	W
C-H γ + O-H γ	2727.44	VW
C=C γ + C=O γ + δ_{as} NH_3^+ + NO_2 γ_{as} + N-O γ + NH α	1629.90	S
C=C γ + C=O γ + COO^- γ_{as} + N-H α + δ_{as} NH_3^+ + CO_2^- γ_{as} + N=O γ + NO_2 γ_{as}	1594.22	VS
CH_3 δ_s + CH_2 δ + OH α + C-O γ + C-CHO (skeletal) + COO^- γ_s + NO_2 γ_s	1383.97	M
CH_3 δ (vibrations) + CH_2 δ (vibrations) + C-O γ +O-H α + C-CHO(skeletal)+ COO^- γ_s +C-N γ + NO_2 γ_s + SO_2 γ_{as} +C=S γ	1350.22	S
C-O-C γ + C-CO-C (skeletal) + C-CHO (skeletal) + C-O γ + C-N γ + NH_3^+ α + N-N γ + SO_2 γ_s + C-F γ	1126.47	VW
C-H β +C-O-C γ + OCN(deformation)+O-N γ + C-S γ + C-Cl γ	765.77	W
C-I γ + C-Br γ +C-S γ + S-O γ + O-N=O δ +OCN(deformation)	620.13	M

α, in-plane bending; β, out-of plane bending; γ, stretching; δ, bending; γ_s, symmetric stretching; γ_{as}, asymmetric stretching; δ_s, symmetric bending; δ_{as} - asymmetric bending; M, medium; S, strong; W, weak; VS, very strong; VW, very weak.

Anti-bacterial studies of copper nanoparticles

Nanomaterials are the leading requirement of the rapidly developing field of nanomedicine, bionanotechnology. Nanoparticles usually have better or different qualities than the bulk material of the same element and have immense surface area relative to volume. For centuries, People have used copper for its antibacterial qualities. However, copper nanoparticles have showed anti-bacterial activities more than copper. Minuscule amounts of copper nanoparticles can lend antimicrobial effects to hundreds of square meters of its host material.

Antibacterial activities of copper nanoparticles synthesized by electrolysis were evaluated by Agar disc diffusion method using Mueller hinton agar. ZOI was measured from this microbiology assay. The sample showed diameter of inhibition zone against *E. Coli* 15 mm and *B. megaterium* 5 mm (Figures 7 and 8). In order to disclose the effective factors on their antibacterial activity, many studies have already been focused on the powder characteristics, such as particle size, shape and lattice constant by various researchers.

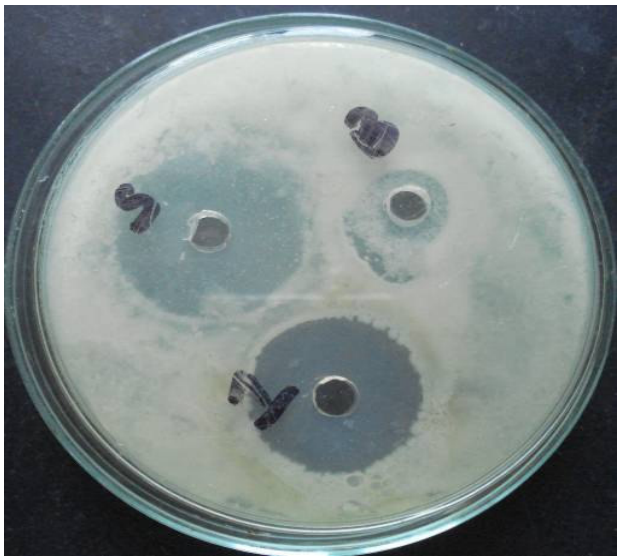

Figure 7. Zone of inhibition diameter against *E. coli* bacteria 15 mm.

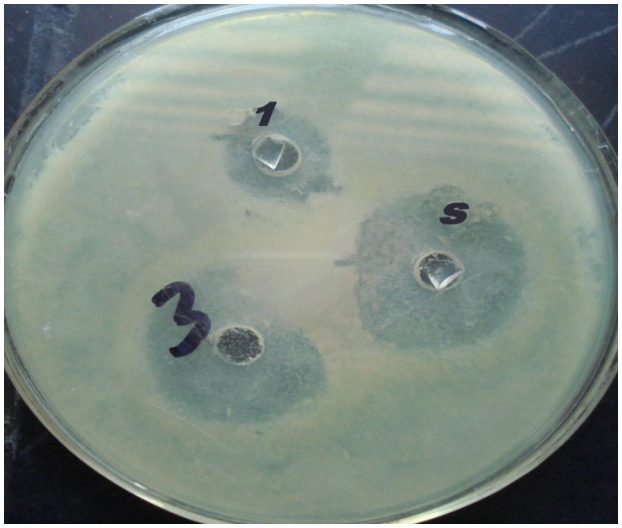

Figure 8. Zone of inhibition diameter against *B. megaterium* 5 mm.

Antibacterial activities evaluation of electrolytic synthesized copper nanoparticles (sample no.1).

In a solid material, the surface-area-to-volume ratio (SA: V) or SSA is an important factor for the reactivity that is, the rate at which the chemical reaction will proceed. Materials with large SA: V (very small diameter) reacts at much faster rates than monolithic materials because more surfaces are available to react.

For studying, changes in SSA of copper nanoparticles and its effects on antibacterial activities of copper nano-particles, we have compared SSA of copper nanoparticles synthesized in electrolysis method with chemical reduction synthesis of copper nanoparticles by Prakash et al. (2009) and the details are in Table 10. From this comparative study, it is noted that antibacterial activities of copper nanoparticles prepared in electrolysis method is more on *E. Coli* (gram negative bacteria) than the copper nanoparticles prepared in chemical reduction synthesis method. It is also noted that increased SSA results in the enhancement of antibacterial activities of copper nanoparticles.

The SSA of cells has an enormous impact on their biology. SSA places a maximum limit on the size of a cell. An increased SSA also means increased exposure to the environment. Greater SSA allows more of the surrounding water to be sifted for nutrients. Increased SSA can also lead to biological problems. More contact with the environment through the surface of a cell increases loss of water and dissolved substances. High SSA also present problems of temperature control in unfavorable environments.

SSA affects the rate at which particles can enter and exit the cell whereas the volume affects the rate at which material are made or used within the cell. These substances must diffuse between the organism and the surroundings. The rate at which a substance can diffuse is given by Fick's law.

$$\text{Rate of Diffusion} \propto \frac{\text{surface area} \times \text{concentration difference}}{\text{distance}} \quad (13)$$

So rate of exchange of substances depends on the organism's surface area that's in contact with the surroundings. Requirements for materials depend on the volume of the organism, so the ability to meet the requirements depends on the SSA.

In addition, we have made an attempt to study the SSA of bacteria and its reactivity to antibacterial activities of copper nanoparticles. For this study, we have compared SSA of *E. coli* with *B. megaterium* and the details are in Table 11. *E. coli* details (Cell length: 2 µm or $2x10^{-6}$ m, diameter: 0.8 µm or $0.8x10^{-6}$ m, total volume: $1x10^{-18}$ m^3, surface area: $6x10^{-12}$ m^2, wet weight: $1x10^{-12}$ g, dry weight: $3.0x10^{-13}$ g) has been extracted from The CyberCell Database- CCDB and SSA calculated accordingly (Shan et al., 2004). SSA of *B. megaterium* has been noted from the research of Reni et al. (1977). From this analysis, we find that *E. coli* has more SSA than *B. megaterium*.

More SSA of *E. coli* increases its exposure to the environment/surroundings in which copper nanoparticles exists and this condition is unfavourable to *E. coli*. It increases rate of exchange of substances that is in contact with the surroundings of *E. coli*. It leads to more reactions of *E. coli* with copper nanoparticles than *B. megaterium*. Due to more reactions in unfavourable surroundings it results in increased zone of inhibition.

Table 10. Comparisons of surface area to volume ratio and antibacterial activities of copper nanoparticles on *E. coli* (gram negative bacteria).

Copper nanoparticles synthesis method	Surface area (nm^2)	Volume (nm^3)	Surface area to volume ratio	SSA (m^2/g)	Diameter inhibition zone (mm)
Electrolysis	1809	7235	0.25	28	15
Chemical Reduction	45216	904320	0.05	5.6	8-10

Table 11. Comparision of bacteria SSA and copper nanoparticles actions.

Bacteria			Copper nanoparticles		
Name	**Variety**	**Specific surface area**	**Inhibition zone diameter**	**Specific surface area**	**Synthesis method**
E. coli	Gram (-)	20.09 m^2/g	15 mm	28 m^2/g	Electrolysis method
B. megaterium	Gram (+)	6.69 m^2/g	5 mm		

Bacteria, viruses and fungi all depend on an enzyme to metabolize oxygen to live. Copper interferes with the effectiveness of the enzyme and disables the uptake of oxygen, thereby killing the microbes. This study reveals that the SSA of bacteria plays a major role while reacting with antimicrobial agents.

Conclusion

In conclusion, we introduce a simple, fast, and economical electrolysis method to synthesize copper nanoparticles. This method provides a clean, nontoxic and eco-friendly and efficient route for the synthesis of nanoparticles with tunable particle size, at room temperature conditions without using any additive. There is no need to use high pressure, energy, temperature, toxic chemicals, downstream processing etc. Handling of the nanoparticles is also much easier than other methods. Based on this study, some other nanoparticles may be prepared in future. From the point of view of nanotechnology, this is a significant advancement to synthesize copper nanoparticles.

The synthesized copper nanoparticles are in spherical shape with particle size of 24 nm. Their characterizations have been successfully done using XRD, SEM and FTIR spectroscopic techniques. Investigation on the antibacterial effect of nanosized copper against *E. coli* and *B. megaterium* microbes reveals high efficacy of copper nanoparticles as a strong antibacterial agent. SSA of copper nanoparticles prepared in two different methods have been analyzed which concludes that increased SSA results in the enhancement of antibacterial activities of copper nanoparticles. Likewise, analysis results of SSA of two different bacteria conclude that SSA of bacteria plays a major role while reacting with antimicrobial agents. These synthesized copper nanoparticles can be useful in food industries, cosmetic industries, medicines and other industries.

ACKNOWLEDGEMENTS

The authors express immense thanks to Dr. G. Venkadamanickam, Rajiv Gandhi Cancer Institute and Research Center, Delhi, India, Dr. M. Palanivelu, Arulmigu Kalasalingam College of Pharmacy (Kalasalingam University, Krishnankoil, India), S. Sivadevi, The SFR College for Women, Sivakasi, India, staff and management of PACR Polytechnic College, Rajapalayam, India and Ayya Nadar Janaki Ammal College, Sivakasi, India for their valuable suggestions, assistances and encouragements during this work.

REFERENCES

Ruparelia.JP, Chatterjee AK, Duttagupta.SP, Mukherji.S (2008). Strain specificity in antimicrobial activity of silver and copper nanoparticles. Acta Biomaterialia, 4(3): 707.

Parameswari E, Udayasoorian C, Paul Sebastian S , Jayabalakrishnan RM (2010). The bactericidal potential of silver nanoparticles. Int. Res. J. Biotechnol., 1(3): 044.

Irshad A, Wani A, Ganguly JA, Ahmad T (2011). Silver nanoparticles: Ultrasonic wave assisted synthesis, optical characterization and surface area studies. Mater. Lett., 65: 520.

Das R, Nath SS, Chakdar D, Gope G, Bhattacharjee R (2009). Preparation of Silver Nanoparticles and Their Characterization. J. Nanotechnol. Online, 5: 1.

Yugang S, Younan Xia (2002). Shape-Controlled Synthesis of Gold and Silver Nanoparticles. Science, 298: 2178.

Xubin P, Iliana Medina-Ramirez, Ray M, Jingbo Liu (2010). Nanocharacterization and bactericidal performance of silver modified titania photocatalyst. Colloids and Surfaces B: Biointerfaces, pp. 77-82. DOI: 10.1016/j.colsurfb.2010.01.010.

Jiji A, Joseph N, Donald RB, Daniel M, Amit S, You Qiang (2006). Size-Dependent Specific Surface Area of Nanoporous Film Assembled by Core-Shell Iron Nanoclusters. J. Nanomater., 54961: 1. DOI: 10.1155/JNM/2006/54961.

Jo-Yong P, Yun-Jo L, Ki-Won J, Jin-Ook Bg, Dae JY (2006). Chemical Synthesis and Characterization of Highly Oil Dispersed MgO

Nanoparticles. J. Ind. Eng. Chem., 12(6): 882.
Prakash N, Jayapradeep S, Sudha PN (2009). Proceeding of ICNM-2009, Appl. Sci. Innovations Pvt. Ltd., India, pp. 311-317.
Shan S, Anchi G, Habibi-Nazhad B, Melania R, Paul S, Michael E, David SW (2004). The CyberCell Database (CCDB): A comprehensive, self- updating, relational database to coordinate and facilitate *in silico* modeling of *Escherichia coli*. Nucleic Acids Res., 32: 293.
Reni S, Elliott B, Gerhardt P (1977). Density, Porosity, and Structure of Dried cell walls Isolated from *Bacillus megaterium* and *Saccharomyces cerevisiae*. J. Bacteriol., 129(2): 1162.